Encoding orbital angular momentum of light in magnets

Hiroyuki Fujita and Masahiro Sato

Phys. Rev. B **96**, 060407 — Published 10 August 2017

DOI: 10.1103/PhysRevB.96.060407

Encoding Orbital Angular Momentum of Lights in Magnets

Hiroyuki Fujita[1, 2, *] and Masahiro Sato[3, 4]

[1] *Institute for Solid State Physics, University of Tokyo, Kashiwa 277-8581, Japan*
[2] *Kavli Institute for Theoretical Physics, University of California, Santa Barbara, CA 93106, USA*[†]
[3] *Department of Physics, Ibaraki University, Mito, Ibaraki 310-8512, Japan*
[4] *Spin Quantum Rectification Project, ERATO, Japan Science and Technology Agency, Sendai 980-8577, Japan*[‡]

(Dated: July 17, 2017)

Breaking the diffraction limit and focusing laser beams to subwavelength scale are becoming possible with the help of recent developments in plasmonics. Such subwavelength focusing bridges different length scales of laser beams and matter. Here we consider optical vortex, or laser beam carrying orbital angular momentum (OAM) and discuss potential subwavelength magnetic phenomena induced by such laser. On the basis of numerical calculations using Landau-Lifshitz-Gilbert equation, we propose two OAM-dependent phenomena induced by optical vortices, generation of radially anisotropic spin waves and generation of topological defects in chiral magnets. The former could lead to the transient topological Hall effect through the laser-induced scalar spin chirality, and the latter reduces the timescale of generating skyrmionic defects by several orders compared to other known means.

PhySH: Angular momentum of light, Ultrafast phenomena, Spin waves, Skyrmions, LLG

Introduction— Realization of ultrashort laser pulses with femto- to pico- second width now offers a powerful tool for the study of non-equilibrium, ultrafast phenomena in solids. Since the pioneering observation of ultrafast demagnetization in Nickel by Beaurepaire et al in 1996 [1], such highly non-equilibrium, laser-induced physics is one of the most important research subjects in the field of magneto-optics [2–16].

So far, most of ultrafast magneto-optical phenomena in solids are explored using laser beams with Gaussian spatial profile. In 1992, however, Allen *et al.* proposed [17] a new type of laser beam, now called optical vortex [18]. Optical vortex is a beam carrying orbital angular momentum (OAM), which can be transferred to physical systems as, for example, mechanical rotation of (semi-) classical particles [19–22]. In the past decades, many applications such as super-resolution microscope [23] and optical ablation [24, 25] are developed. However, the use of optical vortex for controlling microscopic magnetic degrees of freedom of solids is almost unexplored.

The main difficulty in is in the mismatch between the timescales. Typically, the timescale of spin dynamics is in the Tera Hz (THz) or Giga Hz region, but the wavelength of optical vortex of such frequencies is too large for individual spins to "feel" its characteristic spatial profile. Using heating effect, as discussed in Ref. 26 is one option to resolve this issue, but here we take another approach: breaking the diffraction limit [27–30] of THz beams to realize the subwavelencth optical vortices [31]. Stimulated by the enormous successes for the microwave and visible lights, breaking the diffraction limit of THz beams is actively explored and the technologies are rapidly developing recently with the help of plasmonics. We can now design the spatial profile of THz beams at the subwavelength scale [32] and actually focus the THz optical vortices [33] using designed metallic structures such as an array of antennas. Although the technology is still primitive, the prospect for the deep subwavelength focusing of THz beams stimulates studies of ultrafast magnetic phenomena induced by such beams.

In this Rapid Communication, with numerical calculations based on Landau-Lifshitz-Gilbert (LLG) equation, we seek the ultrafast manipulation of magnets through Zeeman and magneto-electric (ME) coupling between spins and the subwavelength optical vortices. We find that optical vortex can be used to excite multipolar and spiral spin waves with OAM dependent wavefronts, which enable us to dynamically generate inhomogeneous spin texture and would induce the transient topological Hall effect [34–39].

Moreover, for chiral ferromagnets with Dzyaloshinskii-Moriya (DM) interaction [40, 41] we observe OAM-dependent generation of topological magnetic defects such as skyrmioniums [5, 42] and skyrmions [43–46], both of which are prospected as ingredients of future magnetic memory devices. We find that OAM of lasers can be transferred as the topological number, i.e. the number of skyrmions generated by the beam. We show that the spatial profile of the subwavelength optical vortex offers an ideal tool for creating skyrmionic defects and the timescale of their generation can be orders of magnitude shorter than other known schemes like heating [26, 47] and electric current pulses [48, 49].

Optical vortex— Optical vortex, or Laguerre-Gaussian (LG) mode is a class of solutions of Maxwell's equations in a vacuum under the paraxial approximation. The derivation of LG modes can be found in literatures [17, 18]. In the cylindrical coordinate (ρ, ϕ, z), where ρ is the radial coordinate and ϕ the azimuthal angle, the field configuration of LG modes propagating in the z direction is given as $\vec{B}(\rho, \phi, z = 0) \propto \vec{e}_p B_{m,p}(\rho, \phi, z = 0)$ at the focal plane ($z = 0$). Here

$\vec{e}_p$ is the polarization vector, $\vec{e}_p = \hat{x}, \hat{y}$ for linearly polarized lights and $\vec{e}_p = \hat{x} \pm i\hat{y}$ for circularly polarized lights. The spatial profile $B_{p,m}$ is characterized by two integers, radial index p and OAM m:

$$B_{m,p}(\rho, \phi, 0) = \left(\frac{\rho}{W}\right)^{|m|} e^{-\frac{\rho^2}{W^2} + im\phi} L_p^{|m|}\left(\frac{2\rho^2}{W^2}\right), \quad (1)$$

where $L_p^{|m|}(\cdot)$ is the generalized Laguerre function.

The non-vanishing phase twist for $m \neq 0$ requires the field to vanish at the topological singularity $\rho = 0$. The beam waist W represents the size of optical vortex (see Fig. 1), and usually cannot be smaller than a half the wavelength because of the diffraction limit. However, as we mentioned, by using plasmonics techniques [27–32], in principle we can take W to be much smaller than the wavelength. In the rest of this paper, we consider the simplest optical vortex with the radial index $p = 0$. We note that LG modes of electric fields, which we consider in the supplementary material, have the same form as magnetic fields presented above, as far as we are discussing the beams propagating in a vacuum.

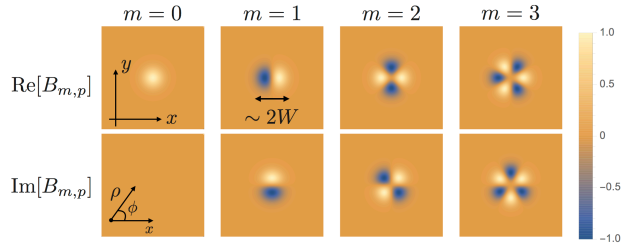

FIG. 1. Snapshots of the spatial profile of magnetic fields of the optical vortex Eq. (1) (for $p = 0$) at the focal plane ($z = 0$) for several values of OAM. For a beam with OAM m, if we go around the topological singularity $\rho = 0$, the magnetic field changes its sign $2m$ times. The peak values of the fields are normalized to unity.

Model and numerical method— In this Rapid Communication, we numerically investigate the laser-driven dynamics of (chiral) ferromagnets. Particularly, in the following, we focus on Zeeman coupling between spins and magnetic fields of optical vortices and study the spin dynamics in the framework of LLG equation. The effect of ME coupling, which can be important and useful in multiferroic materials [50, 51], is discussed in the supplementary material, where we observe qualitatively the same results obtained for Zeeman coupling presented below. Depending on the sign of m, these magnetic field distributions rotate in either clockwise (CW) or counter-clockwise (CCW) way. As we discuss below, the spatially-inhomogeneous in-plane structure of optical vortices shown in Fig. 1 and its time-dependent rotation induce various characteristic phenomena.

Let us consider the situation where a square lattice classical (chiral) ferromagnet is placed at the focal plane of the optical vortex. The Hamiltonian we consider is

$$H = -J\sum_{\vec{r}} \vec{m}_{\vec{r}} \cdot \left(\vec{m}_{\vec{r}+a\vec{e}_x} + \vec{m}_{\vec{r}+a\vec{e}_y}\right) - H_z \sum_{\vec{r}} m^z_{\vec{r}} + \sum_{\vec{r},i} \vec{D}_i \cdot (\vec{m}_{\vec{r}} \times \vec{m}_{\vec{r}+a\vec{e}_i}) - \sum_i \vec{B}(\vec{r}, t) \cdot \vec{m}_{\vec{r}}, \quad (2)$$

where a is the lattice constant and $\vec{e}_i$ is the unit vector along the i-axis ($i = x, y$). The vector $\vec{m}_{\vec{r}}$ represents the spin at the site $\vec{r}$, with its norm normalized to unity. We have the ferromagnetic Heisenberg interaction $J > 0$, DM interaction with DM vector $\vec{D}_i = D\vec{e}_i$ on the bond $(\vec{r}, \vec{r}+a\vec{e}_i)$ [52], and the static external magnetic field applied in the z-direction H_z aside from the optical vortex. The last term describes Zeeman coupling between spins and the optical vortex.

The Hamiltonian Eq. (2) is a canonical model of (chiral) ferromagnets. Despite its simplicity, this model well describes some experimental results of the actual three dimensional (thin film) materials and is widely used for the study of their topological defects, i.e. skyrmions [43–46] (see Ref. 46 for the review). With increasing the external field H_z, the model shows the helical ordered phase, skyrmion lattice phase, and the ferromagnetic phase as observed in thin film materials [53]. In the supplementary material, we give a brief review of this model, the phase diagram and topological defects therein. Depending on the materials, the size of skyrmions can vary from nm to μm [45, 46, 54].

The dynamics of spins under the applied optical vortex is determined by the following LLG equation for the model Eq. (2) [46]:

$$\frac{d\vec{m}_{\vec{r}}}{dt} = -\vec{m}_{\vec{r}} \times \vec{H}_{\text{eff}} + \alpha \vec{m}_{\vec{r}} \times \frac{d\vec{m}_{\vec{r}}}{dt}. \quad (3)$$

The time coordinate t is normalized by $\hbar/J$, which corresponds to 0.13 ps for $J = 5$ meV. The second term in the right hand side of Eq. (3) is the Gilbert damping term describing the dissipation with strength determined by the dimensionless parameter α. We see that each spin precesses around the normalized effective field $\vec{H}_{\text{eff}} = -\vec{\nabla}_{\vec{m}_{\vec{r}}}(H/J)$, and damps towards that. Hereafter, we take $\hbar = J = 1$. Namely, in the following H_z, $\vec{B}$, and $\vec{D}$ are measured in the unit of J, and the time is in the unit of $\hbar/J$.

In the THz region, heating caused by the laser absorption is small, so that we ignore the laser heating effect in the following. Actually, magnetic resonance experiments on magnets and multiferroic materials for THz lights can be well explained by theory without taking the heating effect into account (for example, Refs 55 and 56). In Ref. 55, for an antiferromagnetic dielectric $HoFeO_3$ the temperature change caused by a short intense (~ 1 Tesla) THz magnetic field pulse at the magnetic resonance is estimated to be about 1mK ($< 10^{-4}$ meV). This is orders

of magnitude smaller than the energy scale of the direct coupling between spins and lights.

For the numerical calculations, we use the fourth-order Runge-Kutta method with numerical time step of the calculation $\Delta t = 0.2\hbar/J$. We consider a system consisting of 150 times 150 sites with periodic boundary condition imposed in both x and y directions. In all the cases below, we assume a simple pulse of optical vortex:

$$B(\vec{r},t) = \frac{|B_0|B_{m,p}(\vec{r})}{\max_{\vec{r}}|B_{m,p}(\vec{r})|}\exp\left[-\left(\frac{t-t_0}{\sigma}\right)^2 - i\omega t\right] \quad (4)$$

where ω is the frequency, $|B_0|$ determines the strength of the magnetic field, and σ gives the beam duration. For $J \sim 5$ meV, $B_0 = 0.1$ is about 9 Tesla, $\sigma = 20\hbar/J$ about 3 ps, and $\omega = 1$ about 1.2 THz. In the following, we propose two ultrafast applications of optical vortex, anisotropic spin wave excitations and generation of topological defects. In both cases, below we assume THz optical vortices with nanoscale beam waist $W \sim 10a$, which is orders of magnitude smaller than the wavelength. As we show in the supplementary material and discuss later, even for much larger beam waists, qualitatively the same results can be observed by using proper materials.

Spin waves and magnetic resonance— First we apply optical vortex to ferromagnets with $D = 0$. In this case the sign of OAM is unimportant, but the spatial profile of optical vortices still leads to spin wave excitations with characteristic spatial distribution depending on the value of OAM. Here we only focus on linearly polarized waves $\vec{e}_p = \hat{x}$ with finite OAM. In the supplementary material, we give discussions for circularly polarized optical vortices and Gaussian beams without OAM.

For high frequency beams satisfying $\omega \gtrsim J, H_z$, as shown in Fig. 2, we have multipolar spin waves (dipolar, quadrupolar, octapolar) depending on OAM of the beams. On the other hand, at the magnetic resonance ($\omega \sim H_z$), the spin wave amplitudes become drastically larger, and the multipolar wavefronts connect with each other to be spiral-shaped as shown in Fig. 3. In both cases, the spin structure is modulated from the collinear ferromagnetic state in an inhomogeneous way. Therefore, if (and only if) the laser beam carries OAM, we can dynamically induce the scalar spin chirality $\chi_{i,j,k} = \boldsymbol{S}_i \cdot (\boldsymbol{S}_j \times \boldsymbol{S}_k)$ (j,k are neighboring sites of the site i) as shown in the left-bottom panel of Fig. 3. The non-vanishing net chirality $\chi = \sum_i \chi_{i,i+\hat{y},i+\hat{x}} + \chi_{i,i+\hat{x},i-\hat{y}} + \chi_{i,i-\hat{y},i-\hat{x}} + \chi_{i,i-\hat{x},i+\hat{y}}$ would lead to the topological Hall effect [34–39] in itinerant magnets, but the quantitative analysis is beyond the scope of this paper and may be presented elsewhere.

Generation of topological defects— As we see in Fig. 1, the optical vortex with non-vanishing OAM has radially anisotropic field distribution. This induces either chiral or anti-chiral twist to the spin texture depending on the sign of the OAM. In chiral magnets with $D \neq 0$, such twisted nature of the perturbation should compete with the intrinsic chirality of the magnets determined by their DM interaction.

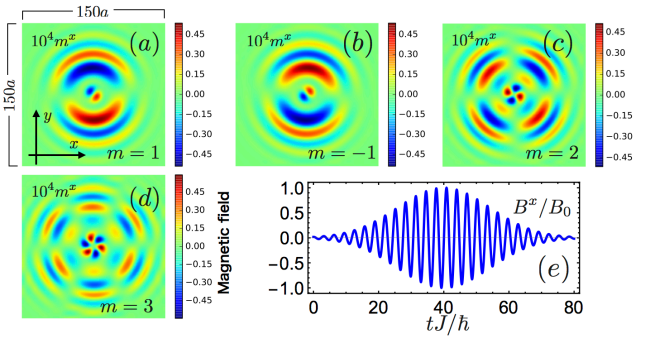

FIG. 2. Multipolar spin wave radiation (a)-(d) induced by linearly polarized optical vortices with $\vec{e}_p = \hat{x}$ for $D = 0$, $H_z = 0.015$, $W = 7.5a$, $\omega = 2$, $\sigma = 20$, $t_0 = 40$, $B_0 = 0.05$, and $\alpha = 0.1$. We show the x-component of spins ($\times 10^4$) at $t = 80$ and the temporal profile of the magnetic field (e) for $m = 1$ at $\rho = w/\sqrt{2}$ and $\phi = 0$. The initial state at $t = 0$ is the ferromagnetic state ($m^z_{\vec{r}} = 1$ for all sites $\vec{r}$). For $J = 5$ meV, $\omega = 2$ corresponds to 2.4 THz and the beam amplitude $B_0 = 0.05$ does 4.3 Tesla.

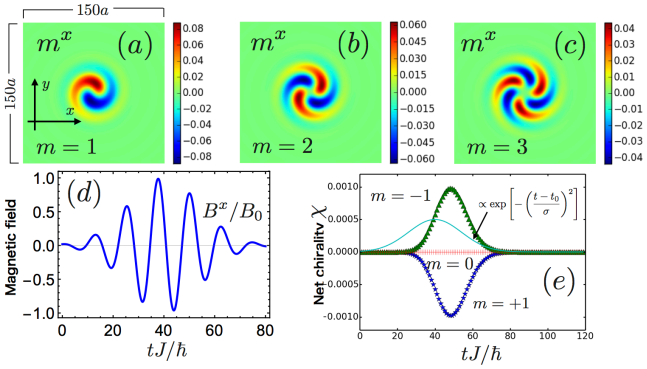

FIG. 3. Spiral spin wave radiation induced by linearly polarized optical vortices (a)-(c) at the magnetic resonance $H_z = \omega = 0.3$ (other parameters are the same as Fig. 2) and the dynamically induced net scalar spin chirality for $m = 0, \pm 1$ (e). Due to the anisotropic spin wave structure, we observe non-vanishing, OAM dependent net scalar spin chirality for $m \neq 0$. We also present the temporal profile of the field (d) for $m = 1$ at $\rho = w/\sqrt{2}$ and $\phi = 0$. For $J = 5$ meV, $\omega = H_z = 0.3$ correspond to 0.4 THz and 26 Tesla.

In the following calculations, we take left-handed optical vortices with polarization vector $\vec{e}_p = \hat{x} + i\hat{y}$. The polarization dependence and the case for Gaussian beams without OAM are discussed in the supplementary material. For left-handed beams, the twist induced to the spin texture by them is CW (CCW) for negative (positive) OAM. Since our model Eq. (2) stabilizes skyrmions with CW spin twisting, for negative OAM chiralities of lights and magnets are in a sense consistent. Here we take the following parameters: $W = 10a$, $\omega = 0.075$,

$\sigma = 10$, $t_0 = 30$, $B_0 = 0.15$, $D = 0.15$, $H_z = 0.015$, and $\alpha = 0.1$ [57]. With these beam parameters, the magnetic field Eq. (4) becomes a half-cycle pulse both for B^x and B^y as shown in Fig. 4, and the beam waist is comparable with the size of skyrmions. For $J \sim 5$ meV, the frequency is about 0.1 THz and the peak values of the fields are about 10 Tesla. We assume the initial state at $t = 0$ to be meta-stable perfect ferromagnetic state in the skyrmion crystal phase of the model Eq. (2). In this phase skyrmionic defects are once formed, stable against weak perturbations such as thermal fluctuations [42] (experimentally skyrmions in some materials can survive even at the room temperature). Hence, even if we take the heating effect ignored in this paper into account, the following results will hold at least qualitatively.

In Fig. 4, we present the OAM dependence of the dynamics of the laser-irradiated chiral magnet. As we noted, in the present setup, $m < 0$ optical vortex twists the spin texture in a way consistent with the intrinsic chirality of the target. In combination with the topological singularity ($\rho = 0$) where the field amplitude is zero, this results in the generation of skyrmioniums for $m = -1$. Due to the destructive effect of the frequent changes in the sign of magnetic fields around the topological singularity, for $m < -1$ we do not obtain skyrmionium. Nevertheless, the OAM dependence of the outcome is clear: the number of skyrmions after the irradiation is given by $\mathrm{sign}(m)(m+1)$. Therefore, we can encoded OAM of optical vortices chiral magnets as their topological charge. Although the field strength assumed here is strong as THz beams, the field enhancement accompanied by the subwavelength focusing [30] would resolve this issue.

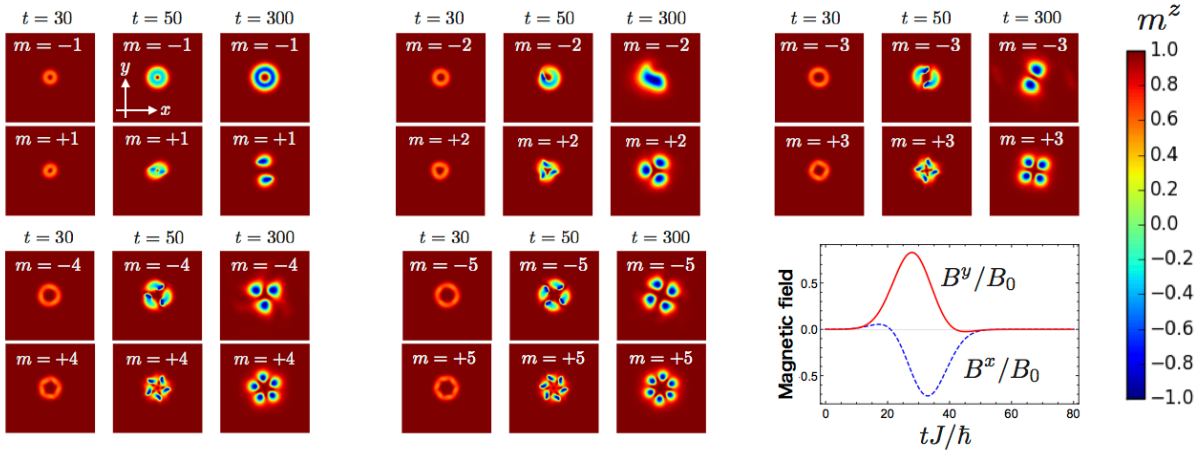

FIG. 4. Orbital angular momentum dependent responses against left-handed beams with $\vec{e}_p = \hat{x} + i\hat{y}$. The initial state at $t = 0$ is the ferromagnetic state where all spins point to the $+\hat{z}$ direction. For $D = 0.15$, $H_z = 0.015$, $W = 10a$, $\omega = 0.075$, $\sigma = 10, t_0 = 30$, $B_0 = 0.15$, and $\alpha = 0.1$, we show time evolutions of spins for various orbital angular momentum m. We also show the temporal profile of the magnetic fields at $\rho = w/\sqrt{2}$ and $\phi = 0$ for $m = 1$. The system size is $150a$ times $150a$ with periodic boundary. The ring-shaped object in $m = -1$ is a skyrmionium and point-like objects in other cases are skyrmions.

Here we comment on the timescale of the process we discussed. As for the creation of skyrmionium, the timescale of its creation with the present scheme (with $m = -1$ beam) turns out to be much shorter than other schemes, and is essentially unchanged even the size of skyrmions is varied (see the supplementary material). The scheme using heating with vortex beams [26] requires beams with period $\mathrm{O}(100)\hbar/J$ long and that using spin-polarized current [49] needs a pulse with duration of $\mathrm{O}(10^4)\hbar/J$ [58], while with our scheme its creation completes within $\mathrm{O}(10)\hbar/J$ (see more details in the supplementary material). Behind the short timescale, there are two features of optical vortices: coherent coupling with spins and the ϕ-dependent spatial profile, which generate the desired twisted spin texture directly in the THz timescale.

Concluding remarks– In this paper, we proposed two ultrafast magnetic phenomena induced by subwavelength optical vortices. We found that OAM of optical vortex can be encoded in magnets in the form of anisotropic spin waves or topological defects. We show that there appears the non-vanishing net spin chirality due to the anisotropic spin waves, which would lead to the laser-induced topological Hall effect. With regard to topological defects in chiral magnets our findings offer a scheme for the ultrafast generation of them. Unlike other known schemes, our method can generate multiple skyrmions at the same time in a controlled way.

Finally, we comment on the experimental feasibility of the proposed phenomena. First, the excitation of the anisotropic spin waves in Figs. 2 and 3 are rather easy, since they are long-wavelength phenomena by nature and do not actually require the subwavelength focusing. On the other hand, the feasibility of the generation of topological defects in Fig. 4 is more subtle. As we mentioned in the introductory part, the THz focusing is at the very

early stage of its study, and at present the maximum focusing achieved experimentally is by a factor of three to four [33], and it is indeed quite challenging to realize the "nanometre" scale focusing we assumed in Fig. 4. However, as discussed in the supplementary material, we can verity that the proper beam waist for the proposed phenomena simply scales with the intrinsic length scale of the target materials, the size of skyrmions. Therefore, by using materials with large skyrmions discovered recently [54, 59–64], the requirement for the focusing factor can be drastically relaxed and we could realize the OAM encoding in Fig. 4.

Acknowledgement— We thank Koichiro Tanaka for useful comments. H. F. is supported by Advanced Leading Graduate Course for Photon Science (ALPS) of Japan Society for the Promotion of Science (JSPS) and JSPS KAKENHI Grant-in-Aid for JSPS Fellows Grant No. JP16J04752. M. S. was supported by Grant-in-Aid for Scientific Research on Innovative Area, Nano Spin Conversion Science (Grant No.17H05174), and JSPS KAKENHI (Grant No. 17K05513 and No. 15H02117). This research was supported in part by the National Science Foundation under Grant No. NSF PHY-1125915. H.F. thanks SPICE, JGU Mainz, where some of the calculations were performed.

* Corresponding author
† h-fujita@issp.u-tokyo.ac.jp
‡ masahiro.sato.phys@vc.ibaraki.ac.jp

[1] E. Beaurepaire, J.-C. Merle, A. Daunois, and J.-Y. Bigot, Phys. Rev. Lett. **76**, 4250 (1996).
[2] A. Kirilyuk, A. V. Kimel, and T. Rasing, Rev. Mod. Phys. **82**, 2731 (2010).
[3] C. D. Stanciu, F. Hansteen, A. V. Kimel, A. Kirilyuk, A. Tsukamoto, A. Itoh, and T. Rasing, Phys. Rev. Lett. **99**, 047601 (2007).
[4] T. Satoh, Y. Terui, R. Moriya, B. A. Ivanov, K. Ando, E. Saitoh, T. Shimura, and K. Kuroda, Nat. Photon. **6**, 662 (2012).
[5] M. Finazzi, M. Savoini, A. R. Khorsand, A. Tsukamoto, A. Itoh, L. Duò, A. Kirilyuk, T. Rasing, and M. Ezawa, Phys. Rev. Lett. **110**, 177205 (2013).
[6] A. D. Caviglia, M. Först, R. Scherwitzl, V. Khanna, H. Bromberger, R. Mankowsky, R. Singla, Y.-D. Chuang, W. S. Lee, O. Krupin, W. F. Schlotter, J. J. Turner, G. L. Dakovski, M. P. Minitti, J. Robinson, V. Scagnoli, S. B. Wilkins, S. A. Cavill, M. Gibert, S. Gariglio, P. Zubko, J.-M. Triscone, J. P. Hill, S. S. Dhesi, and A. Cavalleri, Phys. Rev. B **88**, 220401 (2013).
[7] R. V. Mikhaylovskiy, E. Hendry, A. Secchi, J. H. Mentink, M. Eckstein, A. Wu, R. V. Pisarev, V. V. Kruglyak, M. I. Katsnelson, T. Rasing, and A. V. Kimel, Nat. Commun. **6**, 8190 (2015).
[8] R. R. Subkhangulov, R. V. Mikhaylovskiy, A. K. Zvezdin, V. V. Kruglyak, T. Rasing, and A. V. Kimel, Nat. Photon. **10**, 111 (2016).
[9] M. Sato, Y. Sasaki, and T. Oka, arXiv:1404.2010 (2014).
[10] S. Takayoshi, H. Aoki, and T. Oka, Phys. Rev. B **90**, 085150 (2014).
[11] S. Takayoshi, M. Sato, and T. Oka, Phys. Rev. B **90**, 214413 (2014).
[12] J. H. Mentink, K. Balzer, and M. Eckstein, Nat. Commun. **6**, 6708 (2015).
[13] A. Pimenov, A. A. Mukhin, V. Y. Ivanov, V. D. Travkin, A. M. Balbashov, and A. Loidl, Nature Phys. **2**, 97 (2006).
[14] M. Mochizuki and N. Nagaosa, Phys. Rev. Lett. **105**, 147202 (2010).
[15] Y. Takahashi, R. Shimano, Y. Kaneko, H. Murakawa, and Y. Tokura, Nature Phys. **8**, 121 (2012).
[16] M. Sato, S. Takayoshi, and T. Oka, Phys. Rev. Lett. **117**, 147202 (2016).
[17] L. Allen, M. W. Beijersbergen, R. J. C. Spreeuw, and J. P. Woerdman, Phys. Rev. A **45**, 8185 (1992).
[18] D. L. Andrews and M. Babiker, eds., *The Angular Momentum of Light* (Cambridge University Press, 2012) cambridge Books Online.
[19] M. E. J. Friese, T. A. Nieminen, N. R. Heckenberg, and H. Rubinsztein-Dunlop, Nature **394**, 348 (1998).
[20] H. He, M. E. J. Friese, N. R. Heckenberg, and H. Rubinsztein-Dunlop, Phys. Rev. Lett. **75**, 826 (1995).
[21] L. Paterson, M. P. MacDonald, J. Arlt, W. Sibbett, P. E. Bryant, and K. Dholakia, Science **292**, 912 (2001).
[22] K. Shigematsu, K. Yamane, R. Morita, and Y. Toda, Phys. Rev. B **93**, 045205 (2016).
[23] S. Bretschneider, C. Eggeling, and S. W. Hell, Phys. Rev. Lett. **98**, 218103 (2007).
[24] K. Toyoda, K. Miyamoto, N. Aoki, R. Morita, and T. Omatsu, Nano Lett. **12**, 3645 (2012).
[25] J. Hamazaki, R. Morita, K. Chujo, Y. Kobayashi, S. Tanda, and T. Omatsu, Opt. Express **18**, 2144 (2010).
[26] H. Fujita and M. Sato, Phys. Rev. B **95**, 054421 (2017).
[27] S. A. Maier and H. A. Atwater, J. Appl. Phys. **98**, 011101 (2005).
[28] A. P. Hibbins, J. R. Sambles, C. R. Lawrence, and J. R. Brown, Phys. Rev. Lett. **92**, 143904 (2004).
[29] C.-P. Huang and Y.-Y. Zhu, Act. passive electron. compon. **2007**, 13 (2007).
[30] D. K. Gramotnev and S. I. Bozhevolnyi, Nat. Photon. **4**, 83 (2010).
[31] R. W. Heeres and V. Zwiller, Nano Lett. **14**, 4598 (2014).
[32] S. Morimoto, T. Arikawa, F. Blanchard, K. Sakai, K. Sasaki, and K. Tanaka, in *2016 41st International Conference on Infrared, Millimeter, and Terahertz waves (IRMMW-THz)* (2016) pp. 1–3.
[33] T. Arikawa, S. Morimoto, and K. Tanaka, Opt. Express **25**, 13728 (2017).
[34] J. Ye, Y. B. Kim, A. J. Millis, B. I. Shraiman, P. Majumdar, and Z. Tešanović, Phys. Rev. Lett. **83**, 3737 (1999).
[35] K. Ohgushi, S. Murakami, and N. Nagaosa, Phys. Rev. B **62**, R6065 (2000).
[36] Y. Taguchi, Y. Oohara, H. Yoshizawa, N. Nagaosa, and Y. Tokura, Science **291**, 2573 (2001).
[37] R. Shindou and N. Nagaosa, Phys. Rev. Lett. **87**, 116801 (2001).
[38] G. Tatara and H. Kawamura, Journal of the Physical Society of Japan **71**, 2613 (2002).
[39] A. Neubauer, C. Pfleiderer, B. Binz, A. Rosch, R. Ritz, P. G. Niklowitz, and P. Böni, Phys. Rev. Lett. **102**, 186602 (2009).

[40] I. Dzyaloshinsky, J. Phys. Chem. Solids **4**, 241 (1958).
[41] T. Moriya, Phys. Rev. **120**, 91 (1960).
[42] A. Bogdanov and A. Hubert, J. Magn. Magn. Mater. **138**, 255 (1994).
[43] A. N. Bogdanov and C. Pfleiderer, Nature **442**, 797 (2006).
[44] S. Mühlbauer, B. Binz, F. Jonietz, C. Pfleiderer, A. Rosch, A. Neubauer, R. Georgii, and P. Böni, Science **323**, 915 (2009).
[45] A. Fert, V. Cros, and J. Sampaio, Nat. Nanotechnol. **8**, 152 (2013).
[46] S. Seki and M. Mochizuki, *Skyrmions in Magnetic Materials* (Springer, 2016).
[47] W. Koshibae and N. Nagaosa, Nat. Commun. **5**, 5148 (2014).
[48] H. Y. Yuan and X. R. Wang, Sci. Rep. **6**, 22638 (2016).
[49] X. Zhang, J. Xia, Y. Zhou, D. Wang, X. Liu, W. Zhao, and M. Ezawa, Phys. Rev. B **94**, 094420 (2016).
[50] S.-W. Cheong and M. Mostovoy, Nat. Mater. **6**, 13 (2007).
[51] Y. Tokura, S. Seki, and N. Nagaosa, Rep. Prog. Phys. **77**, 076501 (2014).
[52] With this choice of DM vectors, we obtain so-called Bloch-type skyrmions.
[53] X. Z. Yu, Y. Onose, N. Kanazawa, J. H. Park, J. H. Han, Y. Matsui, N. Nagaosa, and Y. Tokura, Nature **465**, 901 (2010).
[54] K. Shibata, X. Z. Yu, T. Hara, D. Morikawa, N. Kanazawa, K. Kimoto, S. Ishiwata, Y. Matsui, and Y. Tokura, Nat. Nanotechnol. **8**, 723 (2013).
[55] Y. Mukai, H. Hirori, T. Yamamoto, H. Kageyama, and K. Tanaka, New J. Phys. **18**, 013045 (2016).
[56] M. Mochizuki, N. Furukawa, and N. Nagaosa, Phys. Rev. Lett. **104**, 177206 (2010).
[57] We confirm that distinct behaviors between positive and negative OAM is not an artifact of fine-tuning by performing calculations with slightly different beam profiles.
[58] They apply spin-polarized current of a few hundred pico seconds for the exchange coupling 15 pJ/m, which would correspond to $J = 10 - 100$ meV.
[59] W. Jiang, P. Upadhyaya, W. Zhang, G. Yu, M. B. Jungfleisch, F. Y. Fradin, J. E. Pearson, Y. Tserkovnyak, K. L. Wang, O. Heinonen, S. G. E. te Velthuis, and A. Hoffmann, Science **349**, 283 (2015).
[60] G. Yu, P. Upadhyaya, X. Li, W. Li, S. K. Kim, Y. Fan, K. L. Wong, Y. Tserkovnyak, P. K. Amiri, and K. L. Wang, Nano Lett. **16**, 1981 (2016).
[61] S. Woo, K. Litzius, B. Kruger, M.-Y. Im, L. Caretta, K. Richter, M. Mann, A. Krone, R. M. Reeve, M. Weigand, P. Agrawal, I. Lemesh, M.-A. Mawass, P. Fischer, M. Klaui, and G. S. D. Beach, Nat. Mater. **15**, 501 (2016).
[62] C. Moreau-Luchaire, C. Moutafis, N. Reyren, J. Sampaio, C. A. F. Vaz, N. Van Horne, K. Bouzehouane, K. Garcia, C. Deranlot, P. Warnicke, P. Wohlhüter, J. M. George, M. Weigand, J. Raabe, V. Cros, and A. Fert, Nat. Nanotechnol. **11**, 444 (2016).
[63] O. Boulle, J. Vogel, H. Yang, S. Pizzini, D. de Souza Chaves, A. Locatelli, T. O. Menteş, A. Sala, L. D. Buda-Prejbeanu, O. Klein, M. Belmeguenai, Y. Roussigné, A. Stashkevich, S. M. Chérif, L. Aballe, M. Foerster, M. Chshiev, S. Auffret, I. M. Miron, and G. Gaudin, Nat. Nanotechnol. **11**, 449 (2016).
[64] W. Jiang, X. Zhang, G. Yu, W. Zhang, X. Wang, M. Benjamin Jungfleisch, J. E. Pearson, X. Cheng, O. Heinonen, K. L. Wang, Y. Zhou, A. Hoffmann, and S. G. E. te Velthuis, Nature Phys. **13**, 162 (2017).